Activation of Triplet Dioxygen by Glucose Oxidase: Spin−Orbit Coupling in the Superoxide Ion

ARTICLE *in* THE JOURNAL OF PHYSICAL CHEMISTRY B · MARCH 2002

Impact Factor: 3.3 · DOI: 10.1021/jp014013q

4 AUTHORS, INCLUDING:

Boris Minaev
Черкаський національний університ...
328 PUBLICATIONS **3,193** CITATIONS
SEE PROFILE

Hans Agren
KTH Royal Institute of Technology
867 PUBLICATIONS **18,572** CITATIONS
SEE PROFILE

Activation of Triplet Dioxygen by Glucose Oxidase: Spin−Orbit Coupling in the Superoxide Ion

Rajeev Prabhakar,[†] Per E. M. Siegbahn,*[,†] Boris F. Minaev,[‡] and Hans Ågren[‡]

Department of Physics, Stockholm Center for Physics, Astronomy, and Biotechnology (SCFAB), Stockholm University, S-106 91 Stockholm, Sweden, and Laboratory of Theoretical Chemistry, The Royal Institute of Technology, SE-10044 Stockholm, Sweden

Received: October 31, 2001; In Final Form: January 15, 2002

Hybrid density functional calculations have been performed for the reductive activation of dioxygen by glucose oxidase, for which recent experiments have shown substantial kinetic ^{18}O isotope effects but no deuterium isotope effect. The present analysis of the mechanism suggests that this surprising isotope effect is best explained if the rate-determining step is the triplet → singlet interconversion that follows after the electron transfer and the superoxide ion production. The oxygen isotope effect is rationalized by an analysis of the spin−orbit coupling in the radical pair $M^{\bullet+}\cdots O_2^{\bullet-}$, where M is the $FADH_2$ cofactor. For the electron transfer between the M and O_2, the presence of the protonated His516 plays a crucial role by strongly increasing the electron affinity of O_2, which makes the electron transfer exothermic and allows it to occur without any barrier. The chemical step where hydrogen peroxide is formed has a computed free-energy barrier of only 6.6 kcal/mol.

I. Introduction

Dioxygen, O_2, is used as an oxidant in the respiration of mammals and in oxidative metabolic processes, reducing food to water, carbon dioxide, and nitrogen.[1,2] The advantages of aerobic life and oxidative metabolism have been important factors in evolution; these advantages are mainly connected with the high exothermicity of the oxidation of organic molecules. At the same time, aerobic life strongly depends on the kinetic barriers of the molecular oxygen reactions. Although the oxidative transformations of food and respiration are equivalent to that of combustion, the oxygenase enzymes control the specific reaction pathways that store and smoothly release energy, whereas combustion is a radical chain process that requires a high-temperature initiation step.[2] With the strong thermodynamic driving force, it is very important to understand the kinetic constraints that allow the controlled use of dioxygen by aerobic life. The oxygen molecule possesses a triplet ground state, $X^3\Sigma_g^-$, that provides paramagnetic properties of gas-phase dioxygen. Even though Faraday's discovery of this paramagnetism of molecular oxygen was made before 1848, the connections between the paramagnetic nature of the O_2 molecule, its sluggish reactivity, and O_2 involvement in respiration are still not completely understood.[2] A concerted insertion of the ground-state dioxygen into organic (diamagnetic) molecules is a spin-forbidden process. Such limited reactivity is essential for biosynthetic processes; otherwise, dioxygen would burn the substrates rather than supply energy in a controlled way.

Biological systems activate triplet dioxygen for controlled chemical synthesis via electron-transfer and proton-transfer reduction. Dioxygen generally undergoes reactions in a stepwise manner via formation of free-radical intermediates with one unpaired electron:[1,2]

$$O_2 + e^- \rightarrow O_2^- \quad (1)$$

$$O_2^- + H^+ \rightarrow HO_2 \quad (2)$$

$$HO_2 + H^+ + e^- \rightarrow H_2O_2 \quad (3)$$

After production of the first diamagnetic species (eq 3), the following steps do not depend on spin correlation in the radicals:

$$H_2O_2 + H^+ + e^- \rightarrow H_2O + OH \quad (4)$$

$$OH + H^+ + e^- \rightarrow H_2O \quad (5)$$

Although dioxygen is a strong oxidant at pH 7 (when it is a concerted four-electron-transfer agent), it is a weak one-electron oxidant.[2] In terms of the reduction potential, the limiting step is the first electron transfer to O_2. Electron sources in the enzyme that are adequate for the reduction of dioxygen will produce all the other reduced forms via reduction (eq 1), hydrolysis, and disproportionation steps (eqs 2−5).

One important aspect of eqs 1−5 is the coupling of proton- and electron-transfer steps emphasized in numerous studies.[1,2] Another important aspect of dioxygen activation has so far not been addressed sufficiently: if there is a closed-shell cofactor (like $FADH_2$ in glucose oxidase) that is an electron source for the reduction of dioxygen, then production of the closed-shell species is spin-forbidden. After the electron-transfer step (eq 1), the radical pair $M^{\bullet+}\cdots O_2^{\bullet-}$ is produced in the triplet state, where M is the electron donor. The proton transfer (eq 2) does not change the spin multiplicity of the electronic system, but at the stage of hydrogen peroxide production (eq 3), the system is in a ground singlet state. Thus, the triplet → singlet (T → S) spin flip has to occur somewhere during this transformation.

* Corresponding author. E-mail: ps@physto.se.
[†] Stockholm University.
[‡] The Royal Institute of Technology.

10.1021/jp014013q CCC: $22.00
Published on Web 03/19/2002

The T−S transitions in radical pairs have been studied in connection with chemically induced dynamic nuclear- and electron-spin polarization. Chemically induced dynamic nuclear-spin polarization (CIDNP) demonstrates the role of S−T transitions in radical recombination reactions.[3] The non-equilibrium population of the nuclear-spin sublevels pumped during a chemical reaction is usually treated in the framework of the radical pair (RP) theory; S−T mixing is induced by very weak hyperfine coupling and by Zeeman interaction determined through the difference of the *g* factors in separated RPs before the chemical interaction occurs.[3] A similar RP mechanism could be applied for diradicals with long flexible chains, while for the short chain diradicals that are usually produced in organic photochemistry, the S−T transitions are determined mostly by direct spin−orbit coupling (SOC) between the singlet and triplet states.[4,5]

Spin-correlated radical pairs are known to be generated as short-lived intermediates in the primary energy conversion steps of photosynthesis.[6−9] For example, in green plant photosystem I, the RP is generated by electron transfer from the excited singlet state of the primary chlorophyll, P_{700}, to a phylloquinone acceptor, A_1.[7,9] The RP $P_{700}^{\bullet+}A_1^{\bullet-}$ has been detected by time-resolved EPR,[7] which exhibits electron-spin polarization and quantum beats.[9] The theory of this spin polarization[8,9] is based on hyperfine interaction in the $P_{700}^{\bullet+}$ radical, on spin−spin interaction, and on *g*-factor anisotropy in the RP. The interactions are responsible for the S−T evolution in the RP and also for the spin polarization observed. SOC is not considered in this theory,[8,9] which is quite natural for a pure RP with single topicity.[4]

In the RP produced by electron transfer from $FADH_2$ to O_2 in glucose oxidase, the distance between the spins is very long, thus the S and T states are almost perfectly degenerate. This RP formally satisfies the radical pair theory requirement: two spins weakly interact by exchange and by spin−spin dipole interactions. The SOC matrix element should be equal to zero if both radicals have a topicity number equal to 1. But this is not the case for O_2^-. The superoxide anion is a radical with a topicity number equal to 2. It has nonzero orbital angular momentum ($X^2\Pi_g$) that is not quenched completely in the RP. Thus, neither the Salem−Rowland theory[10] nor the radical pair theory of CIDNP[3] can be applied to the RP of the type $M^{\bullet+}\cdots O_2^{\bullet-}$.

The ground state of O_2 can be represented by a single configuration

$$^3\psi_0[X^3\Sigma_g^-] = A(1\sigma_g)^2(1\sigma_u)^2(2\sigma_g)^2(2\sigma_u)^2(3\sigma_g)^2(\pi_u)^4(\pi_g)^2 \quad (6)$$

A spin flip in dioxygen induced by thermal activation is not possible because the excited singlet state, $a^1\Delta_g$, has an excitation energy of 22 kcal/mol but the SOC matrix element between the ground triplet state and $a^1\Delta_g$ is equal to zero by symmetry. Heating alone cannot induce the $X^3\Sigma_g^- \rightarrow a^1\Delta_g$ transition, not because of the high activation energy but because of the strong spin prohibition.[11] Chemical activation along the concerted reaction path is also inefficient for the nonradiative T−S transition initiation in dioxygen.[12,13] For the concerted reaction $O_2 + H_2 = H_2O_2$, the T−S crossing is accompanied by a relatively strong SOC but needs too much activation energy to compete with other processes.[12] Dioxygen interaction with unsaturated hydrocarbons leads to an intermediate biradical, but SOC at the biradical stage is negligible because the T and S states have a similar orbital structure.[4] In the following, it will be shown that the only effective way to overcome spin prohibition and to make dioxygen reactive with respect to a diamagnetic species without a radical chain initiation process (and without spin catalysis by paramagnetic metal ions) is to involve the charge-transfer process in the first elementary step. At the stage of superoxide ion production (O_2^-) by electron transfer from the organic donor molecule (M), a relatively strong probability of electron-spin flip (the triplet → singlet nonradiative transition) occurs in the radical pair $M^{\bullet+}\cdots O_2^{\bullet-}$.[14] The mechanism of the strong SOC enhancement at this stage is similar in nature to the mechanism for the singlet $a^1\Delta_g$ oxygen quenching by amines in the gas phase by charge-transfer contributions.[14,15] Its origin comes from SOC in the $O_2^{\bullet-}$ moiety: the electron spin in the donor radical ion $M^{\bullet+}$ moiety is passive in this radical pair, and the triplet → singlet transition occurs by the spin flip in the superoxide ion moiety of the RP.

The superoxide ion (O_2^-) has been extensively studied in ionic crystals as a color center[16,17] and in solutions.[18] It has also been observed in gas discharges, where it is easily formed by O_2 interaction with free electrons at low energy;[18] at higher energy, O_2^- is indicated by narrow electron-scattering resonances.[17] The superoxide ion has been detected by mass spectrometry in $H_2 + O_2$ mixtures at low pressure.[18] It is formed also in the D layer of the upper atmosphere.[19] Finally, O_2^- is a very important intermediate in dioxygen-utilizing enzymes.[1] Despite its importance, there have been only a few theoretical studies of O_2^-.[17,20,21] Besides the potential energy curves for a number of low-lying states,[17,20,21] other properties of the superoxide ion have not been studied by ab initio methods. To our knowledge, the fine-structure constants have not been calculated.

The ground state of O_2^- can be represented by the dominant configuration

$$^2\psi_0[X^2\Pi_g] = A(1\sigma_g)^2(1\sigma_u)^2(2\sigma_g)^2(2\sigma_u)^2(3\sigma_g)^2(\pi_u)^4(\pi_g)^3 \quad (7)$$

Because the superoxide ion has a $(\pi_g)^3$ open-shell configuration (more than half occupied), it has a negative SOC constant $A(X^2\Pi_g) = -160\ cm^{-1}$.[22] This value is crucial for biochemical applications. The connection between the SOC constant $A(X^2\Pi_g)$ and the rate of the intersystem conversion in dioxygen activation by enzymes will be demonstrated below. The problem of the source of the incoming electron is also important in the enzymes that activate dioxygen; atomic displacements along the reaction coordinate that induce electron transfer will also stabilize the produced superoxide ion. As an example, the reductive activation of dioxygen by glucose oxidase from *Aspergillus niger* will be considered by calculations of the most important steps (eqs 1−3) with a simplified model of the active site. As will be shown below, this enzyme is an unusually good example for studying spin transitions involving dioxygen because this step appears to be rate-limiting in this case.

II. Computational Details

The calculations on the mechanism for O_2^- reduction in glucose oxidase were performed in two steps. First, an optimization of the geometry was made using the B3LYP method[23] with a double-ζ d95(1d,1p) basis set, which includes one polarization function on each atom. Open-shell systems were treated using unrestricted B3LYP(UB3LYP). All degrees of freedom were optimized, and the transition states obtained were confirmed to have only one imaginary frequency of the Hessian. In the second step, the B3LYP energy was evaluated for the optimized geometry using the large 6-311+G(2d,2p) basis set, which includes diffuse functions and two polarization functions on each

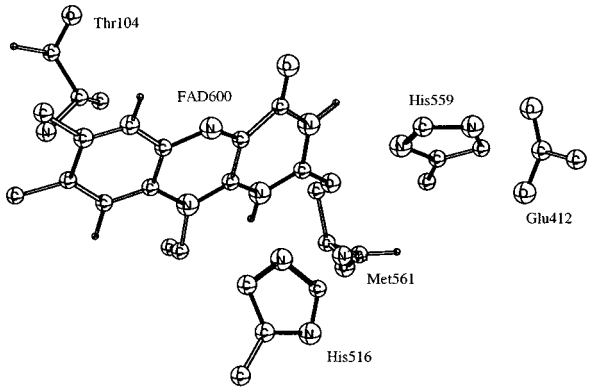

Figure 1. X-ray structure of the active-site region of *Aspergillus niger* glucose oxidase.

atom (see Table 2). Zero-point vibrational effects and thermal effects were added on the basis of B3LYP calculations using the same basis set as that used for the geometry optimization. The dielectric effects from the surrounding environment were obtained using the CPCM polarizable conductor model (Cosmo),[24] where the solvent cavity is formed as a surface of constant charge density of the solvated molecule. The default isodensity value of 0.0004 au is used. The radii of the solvent molecules are taken from the parameters for water. The UAHF (United Atom Topological Model)[25] is used to build the cavity around each atom, and the radius of each atomic sphere is determined by multiplying the van der Waals radius by a scaling factor of 1.2. The dielectric constant was set equal to 4, which corresponds to a dielectric constant of about 3 for the protein and 80 for the water medium surrounding the protein.[26] Because models with the same charge were used throughout the present study, the relative dielectric effects were found to be rather small and not very sensitive to the method used or to the value chosen for the dielectric constant. The relative energies discussed below are Gibbs free energies, where all the effects described above are added. Normal errors involved in using B3LYP and the different aspects of modeling enzyme active sites are described in recent reviews.[27−29] All calculations were performed using the Gaussian 98 program.[30]

III. Mechanism for Hydrogen Peroxide Formation in Glucose Oxidase

Glucose oxidase is a well-studied enzyme,[1] and an X-ray structure from *A. niger* has been determined[31] (see Figure 1). In the active site, there are two histidine residues (His516 and His559) in close proximity to FAD.[31,32] Only His516 has been assigned an important role as the general base in the substrate oxidation.[32] The distance between the protonated nitrogen (N^{ϵ}) of this histidine and the nitrogen atom N1 of the $FADH_2$ ring is 3.8 Å.[31] Dioxygen can occupy the cavity between the $FADH_2$ and His516 moieties. The reaction sequence of glucose oxidase proceeds in two steps: (I) oxidation of glucose to gluconolactone with a simultaneous reduction of the protein-bound cofactor to $FADH_2$ and (II) cycling of $FADH_2$ back to FAD by dioxygen that undergoes reduction to hydrogen peroxide. The reaction in (II) can be written as

$$O_2 + FADH_2 \rightarrow H_2O_2 + FAD \qquad (8)$$

and has been studied here by density functional theory (DFT) using the hybrid B3LYP functional[23] for the model shown in Figure 2. The energies for reaction 8 are given in Table 1, and

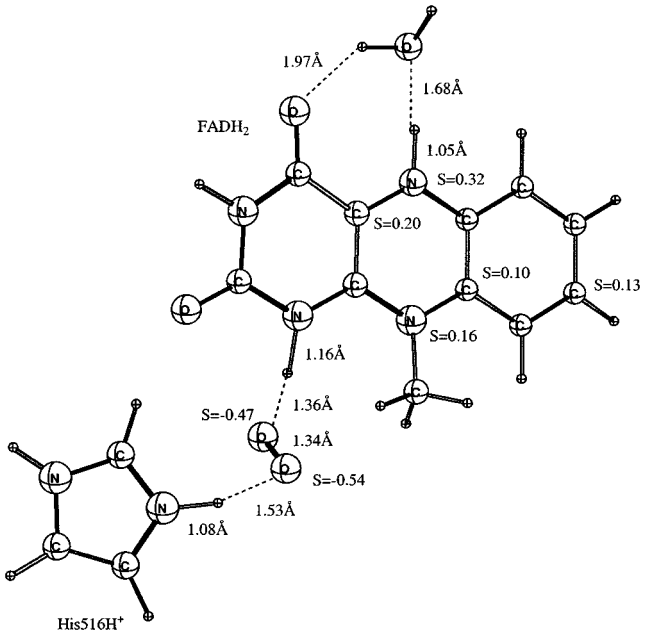

Figure 2. Open-shell singlet product for the first step in glucose oxidase.

TABLE 1: B3LYP Energies (au) for the Reactants and Products of Reaction 8 in Glucose Oxidase

	E_{DZ}	$E_{bigbasis}$
reactants		
$FADH_2$	−794.5610	−794.9217
O_2	−150.3147	−150.3701
products		
FAD	−793.3163	−793.6979
H_2O_2	−151.5405	−151.6054

TABLE 2: Energies (au) for the Optimized Structures in Glucose Oxidase

	$E_{bigbasis}$	$E_{DZ(1d,1p)}$	$E_{\Delta H}$ [a]	E_{solv} [b]	$E_{T\Delta S}$
reactant	−1248.4886	−1248.3322	0.3439	−1248.3816	0.2308
TS	−1248.4742	−1248.3169	0.3393	−1248.3681	0.1394
product	−1248.4924	−1248.3310	0.3435	−1248.3849	0.2322

[a] The sum of zero-point and thermal enthalpy effects. [b] Calculated with the DZ(1d,1p) basis set.

the reaction is calculated to be exothermic by 7.2 kcal/mol without including zero-point, thermal, and dielectric effects.

From the B3LYP calculations, the following mechanism is suggested. In the first step, an electron is transferred from the reduced cofactor $FADH_2$ to dioxygen occupying the small cavity between the N1 and N^{ϵ} atoms. The optimization from the $O_2\cdots M$ starting point leads to the $O_2^{-}\cdots M^{+}$ structure. Thus, the ion−radical pair $M^{\bullet+}\cdots O_2^{\bullet-}$ is generated (see Figure 2). Only the singlet RP is shown in Figure 2 because very similar geometry is obtained for the triplet RP, which is the starting point in the glucose oxidase interaction with triplet dioxygen. It is concluded from DFT calculations that the electron transfer is exothermic and occurs without any activation barrier. The reason for such an easy electron transfer is that the electron affinity (EA) of dioxygen in the presence of a protonated histidine is extremely high, 118.2 kcal/mol from the calculations including dielectric effects. In comparison, the electron affinity of free O_2 in the gas phase is only 10.4 kcal/mol.[22] The presence of the protonated His516 is thus of fundamental importance to the catalytic mechanism of glucose oxidase. The ionization potential (IP) of $FADH_2$ is also quite low, 109.8 kcal/mol from the present calculations including dielectric effects. Neglecting

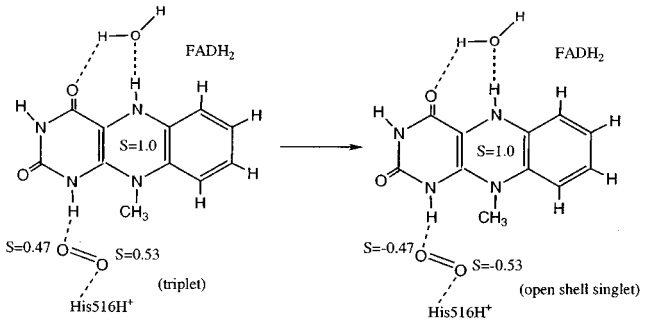

Figure 3. Suggested singlet to triplet transition in glucose oxidase.

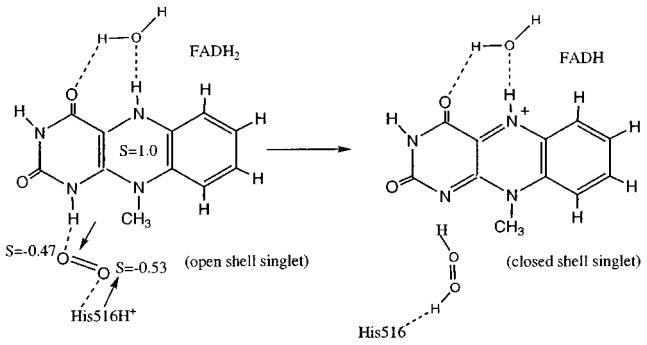

Figure 4. Suggested step for formation of hydrogen peroxide in glucose oxidase.

overlap effects, the energy to form the RP should be approximately equal to IP − EA − Q, where Q is the Coulomb attraction of the two ions. In a simple estimation of Q, it is assumed that the charge is localized at the center of the O_2 molecule and the M cofactor. With a center-to-center distance between O_2 and M of 5.0 Å (approximately 4.6 Å in Figure 2) and a dielectric constant of 4, Q is 16.6 kcal/mol, which means that the electron transfer is estimated to be exothermic by 25.0 kcal/mol. This simple estimate is in agreement with the finding that the radical pair forms exothermically without any barrier in the model calculations. However, this value is quite overestimated because the total available exothermicity is 7.2 kcal/mol for the full reaction 8, and the final proton-transfer step (see below) is calculated to be essentially thermoneutral. This overestimation is due to neglect of electron delocalization in the simple formula. The zeroth vibrational level of O_2 is almost isoenergetic with the $v = 3$ level of the O_2^- ion, and the Franck−Condon factor $|\langle v' = 0|v = 3\rangle|^2$ is relatively large. Thus, the electron-transfer step should be very fast and is not the rate-determining step in the whole process.

The radical pair $M^{\bullet+}\cdots O_2^{\bullet-}$ is generated first in the triplet state because dioxygen is a triplet species and there is no reason to change spin during the electron-transfer process. The electron jump is initiated by the occurrence of dioxygen at the active site and by the weak intermolecular (and O−O) vibrations. To trigger the subsequent chemistry, the triplet → singlet transition has to be induced at the stage of radical pair $M^{\bullet+} \cdots O_2^{\bullet-}$ generation (see Figure 3). When the radical pair is in the singlet state, the $FADH_2^{\bullet+}$ transfers its proton from the N1 nitrogen atom to the $O_2^{\bullet-}$ radical, which is followed by an electron-coupled proton transfer to the O_2H radical, forming H_2O_2 (see Figure 4). The transition state for this $2H^+ + e^-$ transfer process is shown in Figure 5. The calculated free-energy barrier is 6.6 kcal/mol, corresponding to a rate of 10^8 s^{-1}. The reason the process is concerted can be partially understood by the fact that the proton transfer from N1 to the O_2^- radical in the singlet RP $O_2^{\bullet-}\cdots FADH_2^{\bullet+}$ does not need any activation energy because

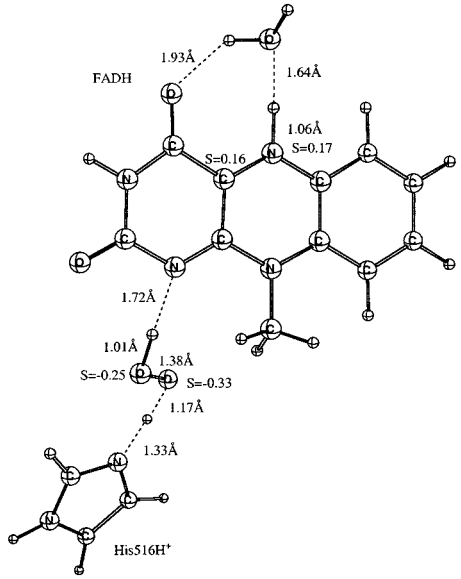

Figure 5. Optimized transition state for formation of hydrogen peroxide in glucose oxidase.

of the $O_2^-\cdots H^+$ attraction and also because no spin change is needed. At the same time, the new nascent singlet radical pair $O_2^{\bullet-}H\cdots FADH_2^{\bullet+}$ creates the perfect condition for an electron-coupled proton transfer, where the electron comes from $FADH_2^{\bullet+}$ and the proton, from $His516H^+$ to the O_2H radical. It must be stressed that such a simultaneous $2H^+ + e^-$ transfer can occur only in the singlet state of the whole system, after which the proton transfer from nitrogen N5 of the flavin ring to the nearest chemical environment (a water molecule in the model in Figure 2) can occur with subsequent proton transfer back to His516. The process $FADH^+ + His \rightarrow FAD + HisH^+$ is calculated to be essentially thermoneutral, endothermic by only 0.6 kcal/mol. Finally, hydrogen peroxide leaves its position in the cavity, and the catalytic cycle is finished. The actual pathway for the final proton-transfer step has not been studied here. The calculated energetics for dioxygen activation in glucose oxidase is shown in Figure 6. It is important to note that while the system undergoes these transformations it remains in the singlet state during both H atom transfer and the subsequent proton-transfer steps.

To obtain the transition state for the $2H^+ + e^-$ process, a molecular Hessian was evaluated. The imaginary frequency of the transition state is 567 cm^{-1}. From the same Hessian, isotope effects, which are extremely important in the present complex, can be evaluated. As mentioned in the Introduction, no deuterium isotope effect is noted experimentally, but a notable oxygen isotope effect is seen instead. For the optimized transition state in Figure 5, the opposite is found—a clear deuterium isotope effect and almost no oxygen isotope effect. Because the isotope effects do not match what is experimentally observed, the step going over the transition state in Figure 5 can therefore not be rate-limiting in glucose oxidase. This conclusion is also in agreement with the rate of 10^8 s^{-1} that was calculated for the process in Figure 5 compared to the experimental rate of only 10^6 s^{-1}.[33] Because the electron transfer from the cofactor to O_2 was found to occur without any barrier, the conclusion drawn here is that the singlet−triplet transition is the rate-limiting step. This is the main conclusion of the present study. The nature of the spin transition is discussed below, including a rationalization for the observed oxygen isotope effect.

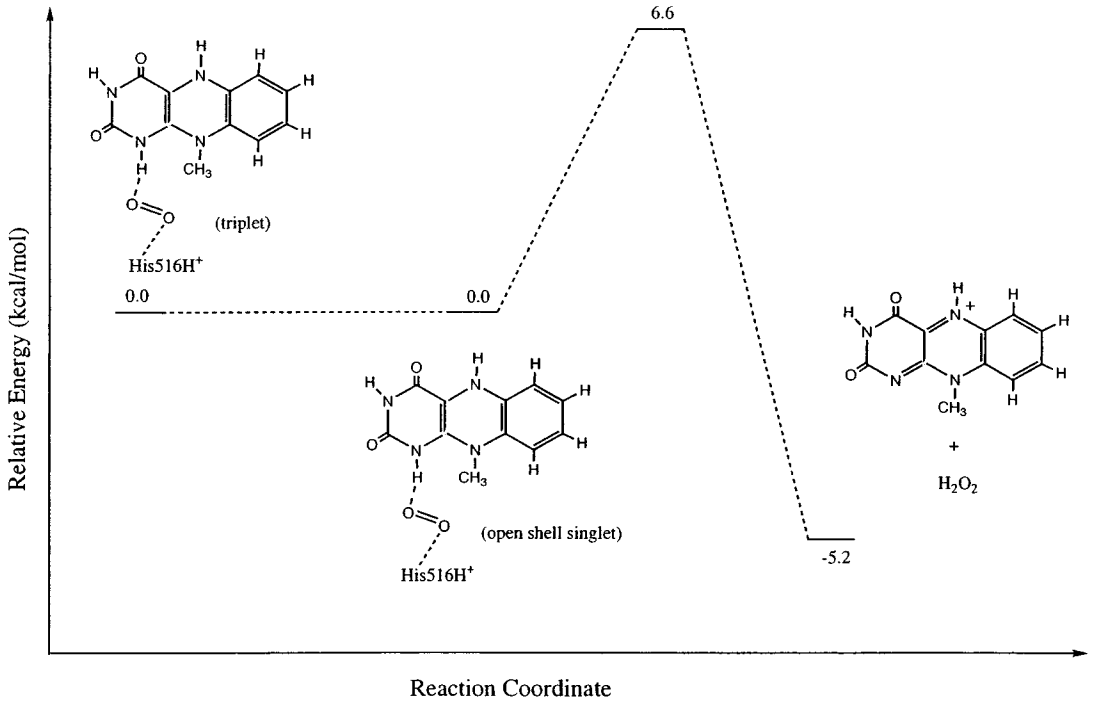

Figure 6. Energy diagram for dioxygen activation in glucose oxidase.

IV. Spin−Orbit Coupling in the Radical Pair $M^{+}\cdots O_2^{-}$

SOC is the main physical factor that allows a molecule to proceed from triplet to singlet states and vice versa. The exact Breit−Pauli form of the SOC operator in molecules is

$$H_{SO} = \frac{\alpha^2}{2}\left(\sum_{i,A} Z_A \frac{\vec{\mathbf{l}}_{iA}\cdot\vec{\mathbf{s}}_i}{r_{iA}^3} - \sum_{ij}\frac{\vec{\mathbf{l}}_{ij}\cdot(\vec{\mathbf{s}}_i + 2\vec{\mathbf{s}}_j)}{r_{ij}^3}\right) \qquad (9)$$

The two-center contributions can be neglected in molecules, to a good approximation. They are of one-electron and two-electron types: both are small and have opposite signs so that they tend to cancel each other. In atoms, the two-electron terms produce important contributions, but they can be accounted for by an effective one-electron operator[34,35]

$$H_{SO} = \zeta_A \sum_i \vec{\mathbf{l}}_i \cdot \vec{\mathbf{s}}_i \qquad (10)$$

where the atomic SOC constant ζ_A can be taken from experimental spectra.

Using this one-electron operator for the ground $X^2\Pi_g$ state of O_2^-, simple algebra leads to the following expression for the splitting of the spin sublevels by the SOC perturbation,

$$E_{1/2} - E_{3/2} = \zeta_O \qquad (11)$$

where the $J = {}^3/_2$ substate is the lowest level. The experimental SOC constant ζ_O for the $O(^3P)$ state is equal to 153 cm^{-1}.[36] Thus, this simple approximation predicts the SOC constant for the ground state of O_2^- to be -153 cm^{-1}, which slightly deviates from the experimental value (-160 cm^{-1}).[22] The deviation can be easily explained by configuration interaction and by the ζ dependence on the effective atomic charge. The energy of the SOC splitting in O_2^- is important to the rate of the spin transition, but it is very small on the thermochemical scale (0.46 kcal/mol).

The estimation of spin−orbit coupling in the radical pair produced by electron transfer from the organic substrate M and dioxygen is naturally much more difficult to make because this is a complicated polyatomic system. As far as SOC is concerned, one has to note that in nonlinear molecules the expectation value of the orbital angular momentum is equal to zero, which does not mean that the SOC effects vanish. The first-order perturbation theory correction (expectation value of the SOC operator) is zero because $\langle L\rangle = 0$. The splitting of the triplet-state spin sublevels in nonlinear molecules like benzene or naphthalene (which has been studied by EPR spectroscopy)[37] is really very small ($\sim$0.2 cm^{-1})[37] because SOC cannot contribute to the splitting in first order and the second-order contributions are negligible for aromatic molecules,[38] which is not the case for the radical pair $M^{+}\cdots O_2^{-}$. The orbital angular momentum of the system is zero, but the second-order SOC contribution to the triplet-state splitting in the radical pair can be large. The intersystem crossing probability, rather than the zero-field splitting of the radical pair, is of particular interest here.

To understand the spin transition involving the superoxide anion, the orbital structure for the electron transfer between an organic substrate M and dioxygen first needs to be considered (see Figure 7). The starting reactants are in the triplet ground state (Figure 7a) because the total spin is determined by the triplet oxygen molecule. The organic substrate M is assumed to be a diamagnetic species in the singlet ground state. Representative states for the radical pair are shown schematically in Figure 7b and c. $^3\Psi_{xb}$ and $^1\Psi_{yb}$ are the lowest states of the RP that was optimized by the DFT method. In a way similar to the formation of $^3\Psi_{xb}$ and $^1\Psi_{yb}$, the low-lying excited states of the RP $^3\Psi_{yb}$ and $^1\Psi_{xb}$ can also be formed. These four configurations are nearly degenerate. The near degeneracy is supported by the B3LYP calculations that give a splitting between the triplet and singlet states (see Figure 2) of only 0.13

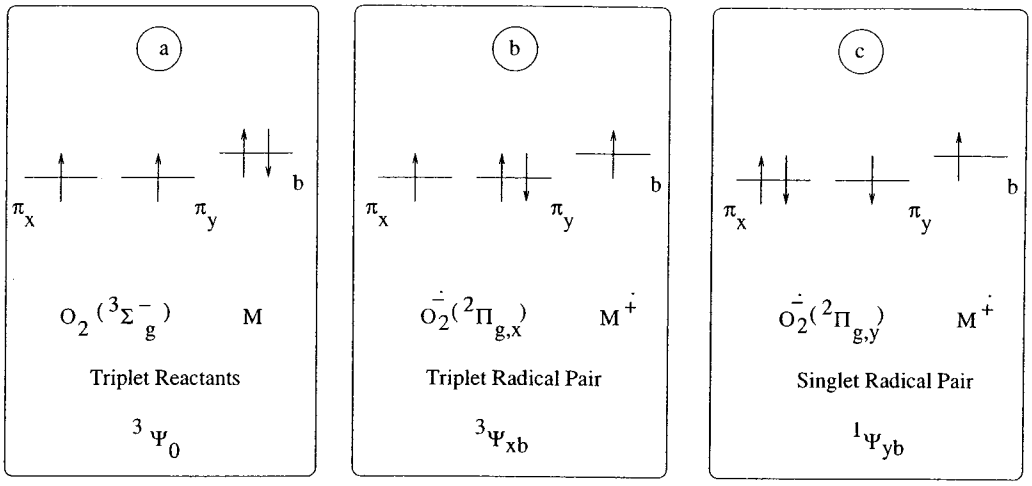

Figure 7. Schematic view of the configurations of the pair dioxygen + cofactor.

kcal/mol. The wave functions of the states, shown in Figure 7, omitting the closed shells, can be written as

$$^3\Psi_0(^3\Sigma_g^- M) = \frac{1}{\sqrt{2}}(|b\bar{b}x\bar{y}| + |b\bar{b}\bar{x}y|) \quad (12)$$

$$^3\Psi_{RP}(O_2^-\cdots M^+) = \frac{1}{\sqrt{2}}(|by\bar{y}\bar{x}| + |\bar{b}y\bar{y}x|) = {}^3\Psi_{xb} \quad (13)$$

$$^1\Psi_{RP}(O_2^-\cdots M^+) = \frac{1}{\sqrt{2}}(|bx\bar{x}\bar{y}| - |\bar{b}x\bar{x}y|) = {}^1\Psi_{yb} \quad (14)$$

where x and y designate the two degenerate π_g MOs of dioxygen and b is the HOMO of $FADH_2^+$. The radical pair in eq 14 is a singlet state with electron transfer from the $FADH_2$ HOMO b to the incompletely filled $\pi_{g,x}$ MO of dioxygen. The triplet-state spin functions in eqs 12 and 13 have a spin projection on the *z* axis equal to zero, $M_S = 0$. It should be noted that there is no preferential direction in the molecule (such as the *z* axis in case of an external magnetic field B_z). In the case of $L = 0$ (a general case for polyatomic nonlinear molecules), a very weak internal magnetic field in the triplet state is created by two parallel spins; a corresponding weak spin−spin interaction leads to a small splitting of the three triplet sublevels. The zero-field splitting (ZFS) of the three sublevels[37] depends on the anisotropy of the two electron clouds, (i.e., the spatial distribution of the two nonpaired electrons), which is why the ZFS and quantization of the spin projection in the triplet state of a polyatomic nonlinear molecule depend on the symmetry of its nuclear skeleton. The axis of the O−O bond can be chosen as the *z* axis in the system M···O_2. In the ground triplet state of the pair, spin−spin interaction in dioxygen determines the axis of the spin quantization. In the RP $M^+\cdots O_2^-$, spin−spin interaction will determine the axis of spin quantization in a more complicated way. However, even though the second-order SOC effect will be much stronger than the spin−spin interaction expectation value, the *z* axis is still preferable as the main ZFS axis. Thus, the triplet states with $M_S = 0$ are most useful and relevant for the present purposes.

The *z* component of the SOC operator for the four-electron system can be written in the form (similar considerations can be made for the *x* and *y* components)

$$H^z_{SO} = \sum_A \zeta_A \sum_{i=1}^{4} l^A_{z,i} s_{z,i} = \sum_{i=1}^{4} B_{z,i} s_{z,i} \quad (15)$$

where $B_{z,i} = \sum_A \zeta_A l^A_{z,i}$ is an orbital part of the SOC operator. The *x* and *y* components of the SOC operator do not contribute to the total SOC integral. It is easy to see that only the crossed matrix elements between, for example, the states in eqs 13 and 14 are important in the intersystem crossing (ISC) of the radical pair $O_2^-\cdots M^+$. The SOC matrix element between these triplet and singlet states is equal to

$$\langle {}^3\Psi_{xb}|H^z_{SO}|{}^1\Psi_{yb}\rangle = -\frac{1}{2}\langle y|B_z|x\rangle = -\frac{i}{2}\zeta_O = -76.5i \text{ cm}^{-1} \quad (16)$$

The SOC matrix element between the crossing S and T states of the RP reaches its largest value at the crossing point (the maximum possible in the system); the SOC is due to the oxygen moiety exclusively (the other atoms of the radical pair do not contribute).

From a comparison to the SOC constant of the $X^2\Pi_g$ state of the O_2^- ion, one can see that the SOC integral in the RP (eq 16) is equal to one-half of the observed SOC splitting in the superoxide ion. Though the result is approximate, there is no reason for an appreciable deviation (more than 1%) from this simple prediction. The rate of the spin transition can be estimated by Fermi's Golden Rule

$$k_{TS} = \frac{2\pi}{\hbar}|\langle {}^3\Psi_{xb}|H_{SO}|{}^1\Psi_{yb}\rangle|^2 \rho(E) FC \quad (17)$$

where $\rho(E)$ is the density of the rovibronic states in the final electronic state; this density is Franck−Condon (FC) weighted.[39] Comprehensive descriptions of the important roles of the Franck−Condon factors in spin-transition processes can be found elsewhere.[39−41]

Let us suppose that at the stage of electron transfer the superoxide ion is generated in the $^2\Pi_{g,x}$ state and the radical pair $^3\Psi_{xb}$ appears (Figure 7b). The proton is far away because the N1−H bond is not cleaved yet. When the proton starts to move, the state $^1\Psi_{yb}$ (Figure 7c) becomes more stabilized: the doubly occupied π_x MO is stabilized by overlap with the hydrogen orbital. Thus, the $^3\Psi_{xb}$−$^1\Psi_{yb}$ crossing occurs, and the T → S transition is possible. During this process, the electron jump $\pi_y \rightarrow \pi_x$ occurs (Figure 8), which is equivalent to the orbital rotation in the superoxide ion; this torque creates a magnetic field that finally induces the spin flip (SOC).

The structure of O_2^- in the RP of the enzyme active site is not strongly perturbed by the interaction with the environment

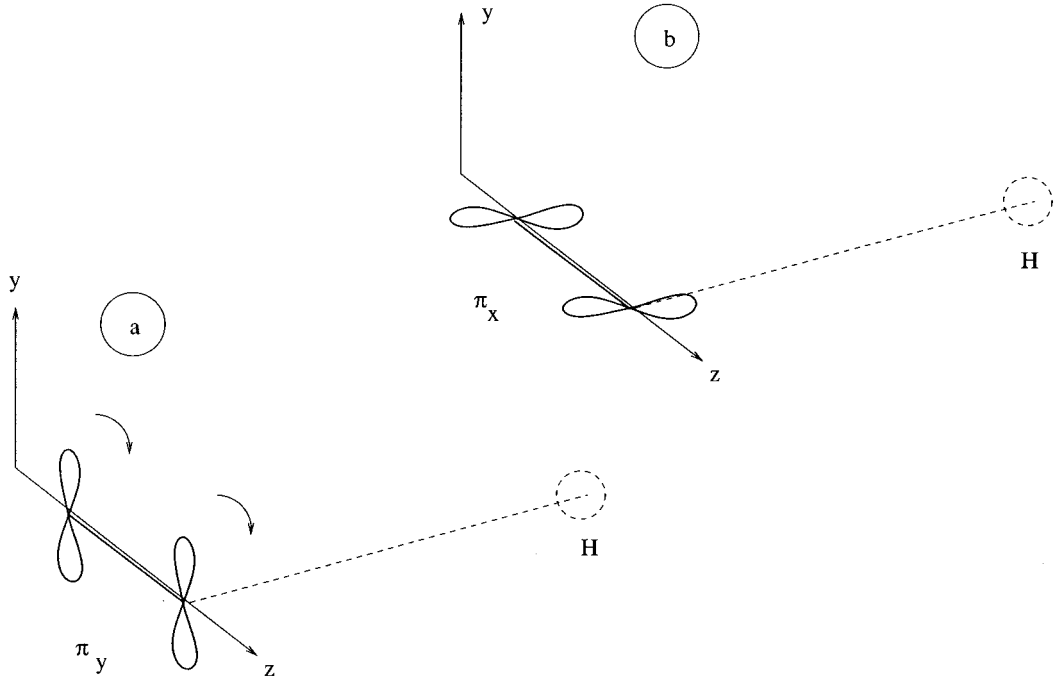

Figure 8. π_x and π_y MOs of the superoxide ion in contact with the N1−H group of the $FADH_2$ cofactor M. The protonated histidine (His516) is omitted here.

TABLE 3: Normal Modes (ω_n) of Promoting Vibrations in Glucose Oxidase (in cm^{-1})

	26.5			76.2			83.4			1278.6		
	x	*y*	*z*	*x*	*y*	*z*	*x*	*y*	*z*	*x*	*y*	*z*
N1	−0.03	0.05	−0.01	−0.02	0.01	0.05	0.04	0.05	−0.04	−0.06	0.07	−0.01
H	−0.03	0.04	−0.02	−0.01	0.03	0.01	−0.03	0.04	0.06	0.27	0.05	0.20
O_1[a]	−0.02	−0.01	−0.07	−0.02	0.01	−0.01	−0.01	0.05	0.16	0.02	0.05	−0.08
O_2[b]	−0.04	0.00	−0.07	−0.01	0.03	0.01	−0.08	0.10	0.16	−0.02	−0.04	0.09
H	0.00	−0.04	−0.03	−0.02	−0.04	−0.02	−0.16	−0.19	−0.08	0.00	−0.15	−0.47
N^{ϵ}	0.00	−0.05	−0.01	−0.02	−0.04	−0.03	−0.15	−0.19	−0.13	0.00	0.01	0.03

[a] O_1 closer to N1. [b] O_2 closer to N^{ϵ}.

of the enzyme, which is indicated by the near degeneracy of the T and S states. The calculated frequency of the O−O vibration in the RP (1278 cm^{-1}) is close to the O_2^- vibrational frequency (1090 cm^{-1}). In O_2^-, the $X^2\Pi_g$ state is doubly degenerate in the absence of SOC, and we can anticipate that the $^3\Psi_{xb}$ and $^3\Psi_{yb}$ are close in energy. Because the electron-transfer reaction energy definitely is higher than the $^3\Psi_{xb}-^3\Psi_{yb}$ energy gap, both states can be populated. Let us suppose that the $^3\Psi_{xb}$ state is produced. In that case, the T → S transition $^3\Psi_{xb} \rightarrow {}^1\Psi_{yb}$ can occur with a relatively large probability, which follows from the SOC analysis, eq 12−16. If the $^3\Psi_{yb}$ state is generated first, then the $^3\Psi_{yb} \rightarrow {}^1\Psi_{xb}$ transition would occur with a similar SOC integral (eq 16) and with similar probability. The main implication of the SOC analysis is that during the T → S transition the electron jump from the Π_y to the Π_x orbital (or vice versa) has to occur. This kind of electronic orbital rotation ($\Pi_y \rightarrow \Pi_x$, Figure 8) creates a torque and a magnetic field (SOC) that finally induce the spin flip during the T → S quantum transition. This qualitative analysis is insufficient, as is any interpretation of a quantum transition in terms of semiclassical concepts and notions, but it is still useful and has been widely used in spectroscopy and photochemistry.[4,13] The T → S transition occurs before the $2H^+ + e^-$ transfer reactions (eq 2, 3), but intermolecular vibrations that promote the T → S transition are connected with the reaction coordinate. From the TS analysis, we know that the process is concerted and that the proton from $FADH_2^+$ to O_2^- moves earlier along the reaction coordinate. It is obvious that the T and S states have different force fields and slightly different vibrational frequencies with respect to the $N-H^+\cdots O_2^-\cdots H-N^+$ intermolecular binding: the S state has a small barrier for $2H^+ + e^-$ transfer (eq 8), but in the T state, such a reaction is highly endothermic because the triplet state of hydrogen peroxide is an excited repulsive state. Thus, the movement along the reaction coordinate produces different curvatures for the S and T potentials. The same is true for intermolecular potentials near equlibrium and for vibrational frequencies. The equlibrium geometries are also slightly different. For example, the N1H···O distance is 1.446 Å in the T state and 1.440 Å in the S state of the radical pair $FADH_2^+\cdots O_2^-$. The shift between the two harmonic oscillator equlibria is small (0.006 Å) but still nonzero. Movement along this intermolecular stretching vibration induces the T−S crossing and is the promoting mode for the T → S transition. Besides this particular vibration, there are four others that are seen as promoting modes: O−O and N^{ϵ} stretchings, the hindered rotation of the O_2^- moiety around the *xy*-bisecting axis, etc. (see Table 3). The hindered O_2^- rotation has a small frequency (83 cm^{-1}); this movement has to make the energies equal for the $^3\Psi_{xb}$ and $^3\Psi_{yb}$ states. At the maximum and minimum points of the amplitude of this vibration, the energy of the two states is interchanged. Thus, it is not important which is the starting point for the electron transfer; the most important fact is that the $^3\Psi_{xb} \rightarrow {}^1\Psi_{yb}$ crossing is induced upon this hindered rotation. The role of the enzyme is to create conditions for the production of the radical pair $O_2^-\cdots M^+$. If the enzyme's chemical environment permits this RP to have a lifetime of about $10^{-4}-10^{-6}$ s, then

the nonradiative T → S transition can definitely occur because the strong SOC in the O_2^- moiety will effectively mix the T and S states. From comparisons with other chemical reactions that are forbidden by the spin selection rule and that are observed with a competitive rate and yield, one can conclude that the SOC matrix element on the order 40−70 cm^{-1} can provide a reasonably efficient T → S transition during the movement along the reaction coordinate, in radical pairs, or in other intermediates.[35] Accounting for the uncertainties in the global Franck−Condon factor and in the variety of intermolecular vibrational modes and their normal coordinates, a lower limit of the T → S transition rate constant can be estimated to be on the order 10^4-10^6 s^{-1}, which should be long enough to allow the transition to occur during the lifetime of the RP. It is interesting to note that this estimated rate is in reasonable agreement with the observed rate of 10^6 s^{-1} for dioxygen reduction in glucose oxidase.[33]

From studies of the emission properties of organic molecules at low temperature in rigid media (under conditions such that bimolecular quenching and thermal collisional deactivation are minimized), the radiative and nonradiative T−S transitions are generally 10^3-10^6 less probable than the corresponding singlet−singlet transitions.[42] 10^6 corresponds to aromatic hydrocarbons where SOC matrix elements between $^3(\pi\pi^*)$ and $^1(\pi\pi^*)$ states do not include one-center integrals and do not exceed 1 cm^{-1}.[35] The largest SOC integrals in organic molecules (nitrogen-containing heterocycles, aldehydes) between T and S states are about 30−40 cm^{-1}, which provide a 1000-fold increase of k_{TS}.[14,43] The maximum possible SOC integral is obtained for dioxygen itself: $\langle X^3\Sigma_g^-|H_{SO}|b^1\Sigma_g^+\rangle = 168$ cm^{-1}.[44] In organic systems containing dioxygen, the largest possible SOC value is realized in the singlet−triplet radical pair $O_2^-\cdots M^+$. This SOC integral does not depend on the nature of the organic radical cation M^+ but is determined by the SOC constant of the $X^2\Pi_g$ state of the O_2^- ion.

As already mentioned, a notable $^{18}O/^{16}O$ isotope effect in the rate-limiting step of glucose oxidase has been reported.[1] The main origin of this effect is the condition that the energies of the singlet and triplet states of the radical pair have to be the same at the position of the spin transition. The energy separation between the states depends mainly on intermolecular modes that modulate the O···M separation. The ISC rate constant (eq 17) is therefore sensitive to the oxygen isotope substitution through the Franck−Condon factors. For each promoting mode, the FC factor in the harmonic approximation can be written as[45]

$$\langle S, 0|T, 0\rangle = (1 - x^2)^{1/4} \exp^{-f^2(1-x)/2} \qquad (18)$$

$$\langle S, 1|T, 0\rangle = (1 - x^2)^{1/4} \exp^{-f^2(1-x)[-f(1-x)]/2} \qquad (19)$$

where

$$x = \frac{\omega_S - \omega_T}{\omega_S + \omega_T}, \qquad f = \sqrt{\frac{\omega_S}{\omega_T}}\eta_{ST}$$

ω_S and ω_T are the vibrational frequencies in the triplet and singlet states, respectively. $\langle S, 1|$ means the first excited vibrational level in the singlet state. The most important FC factor for 1 quantum of the promoting mode (eq 19) is proportional to f and η_{ST}, which is equal to

$$\eta_{ST} = \frac{R_S - R_T}{a\sqrt{2}}, \qquad a = \frac{1}{\sqrt{\mu}\omega_T}$$

where μ is the reduced mass and R_S and R_T are the equilibrium distances. All values are in atomic units. The global FC factor is the product of single-mode values. The FC factor depends on the O^{16}/O^{18} isotope substitution, mostly through the reduced mass. We have used the equilibrium displacement shifts (R_S and R_T) from the O^{16} calculation. The FC factor is changed upon O^{16}/O^{18} substitution because the promoting modes include the O···H−N and O−O stretching. The most important motion is the hindered rotation of O_2^- in the cavity of the enzyme binding site. Rough estimates indicate that a measured isotope effect on the order of 1−2% can be inferred.

V. Conclusions

The present study of the formation of hydrogen peroxide from the triplet O_2 molecule by glucose oxidase can be summarized as follows. The starting point for the investigation is when O_2 is occupying the cavity between $FADH_2$ and the protonated histidine (His516). At this point, a spontaneous exothermic electron transfer is obtained (Figure 2) without any barrier. The reason this electron transfer is exothermic is that His516 next to O_2 is protonated. His516 thus plays a crucial role in dioxygen reduction in glucose oxidase. The triplet RP at this stage undergoes a T−S nonradiative transition (ISC), induced by a relatively strong SOC that originates from SOC in the superoxide moiety of the RP. The organic counterpart ($M^{\bullet+}$) is passive in this SOC mixing. This model can therefore be applied to many similar systems where molecular oxygen is activated by initial electron transfer: SOC between triplet and singlet states of the radical pair $M^{\bullet+}\cdots O_2^{\bullet-}$ does not depend on the nature of the organic electron donor M but is determined by the nearly free orbital rotation in the O_2^- moiety. The crossing between the T and S potential surfaces has to occur at a point where these states have the same energy; therefore, it is affected by intermolecular vibrations that to a large extent involve the O_2^- librational motion and O−O vibrations. Furthermore, the Franck−Condon factors for the respective modes depend on the $^{18}O/^{16}O$ isotope substitution, which means that the nonradiative triplet−singlet transition rate constant will depend on the $^{18}O/^{16}O$ isotope effect. From the experimentally observed dependence of the rate on this isotope effect, it is concluded that this is the rate-limiting step in dioxygen reduction by glucose oxidase. When the radical pair is in a singlet state, the second part of the process is triggered (Figure 4). In glucose oxidase, this process includes first the proton transfer from N1 to the $O_2^{\bullet-}$ radical, followed by an electron-coupled proton transfer where the electron comes from the $FADH_2^{\bullet+}$ and the proton, from the protonated histidine ($His516H^+$) (from N^ϵ to the O_2H radical) (Figure 5). The computed free-energy barrier is only 6.6 kcal/mol. After that, the proton transfer from the nitrogen N5 atom of the flavin ring to the nearest chemical environment (a water molecule in the model in Figure 2) occurs with subsequent proton transfer back to the neutral histidine (His516) through the protein-bound network of hydrogen bonds. The release of H and H^+ from $FADH_2^+$ is made easier by the strong aromatic stabilization of the FAD molecule.

Whenever dioxygen is activated in enzymes, the question of a spin transition must arise. Unlike that in the case of glucose oxidase, this process is simplified for most enzymes by the presence of paramagnetic metal centers. Copper amine oxidases, amino acid hydroxylases, iron dioxygenases, and monooxygenases are examples of such enzymes. In these cases, the triplet → singlet interconversion is influenced both by chemical bonding to the metal and by spin catalysis of the exchange type.

Acknowledgment. This work was supported by the Swedish Royal Academy of Science and the Natural Research Council.

References and Notes

(1) Klinman, J. P. *J. Biol. Inorg. Chem.* **2001**, *6*, 1.
(2) Sawyer, D. T. In *Oxygen Chemistry*; Oxford University: New York, 1991.
(3) Closs, G. L. *J. Am. Chem. Soc.* **1971**, *93*, 1123.
(4) Minaev, B. F. Theoretical Analysis and Prognostication of Spin−Orbit Coupling Effects in Molecular Spectroscopy and Chemical Kinetics (in Russian). Dr. Sc. Thesis, N. N. Semenov Institute of Chemical Physics, Moscow, 1983.
(5) Doubleday, C.; Turro, N. J.; Wang, J. F. *Acc. Chem. Res.* **1989**, *22*, 199.
(6) Thurnauer, M. C.; Norris, J. R. *Chem. Phys. Lett.* **1980**, *76*, 557.
(7) Thurnauer, M. C.; Rutherford, A. W.; Norris, J. R. *Biochim. Biophys. Acta* **1982**, *682*, 332.
(8) Closs, G. L.; Forbes, M. D. E.; Norris, J. R. *J. Phys. Chem.* **1987**, *91*, 3592.
(9) Link, G.; Berthold, T.; Berthold, M.; Weidner, J. U.; Thurnauer, M. C.; Kothe, G. *J. Am. Chem. Soc.* **2001**, *123*, 4211.
(10) Salem, L.; Rowland, C. *Angew. Chem., Int. Ed. Engl.* **1972**, *11*, 92.
(11) Minaev, B. F. *Int. J. Quantum Chem.* **1980**, *17*, 367.
(12) Minaev, B. F. *Sov. J. Chem. Phys.* **1985**, *3*, 1533.
(13) Minaev, B. F.; Ågren, H. *Int. J. Quantum Chem.* **1996**, *57*, 510.
(14) Minaev, B. F. *Theor. Exp. Chem. (USSR).* **1984**, *20*, 199.
(15) Ogryzlo, E. A.; Tang, C. W. *J. Am. Chem. Soc.* **1970**, *92*, 5034.
(16) Rolfe, J. *J. Chem. Phys.* **1979**, *70*, 2643.
(17) Ewig, C. S.; Tellinghuisen, J. *J. Chem. Phys.* **1991**, *95*, 1097.
(18) Krupenie, P. H. *J. Phys. Chem. Ref. Data* **1972**, *1*, 423.
(19) Reid, G. C. *Adv. At. Mol. Phys.* **1976**, *12*, 375.
(20) Das, G.; Zemke, W. T.; Stwalley, W. C. *J. Chem. Phys.* **1980**, *72*, 2327.
(21) Gonzalez-Luque, R.; Merchan, M.; Fülscher, M. P.; Roos, B. O. *Chem. Phys. Lett.* **1993**, *204*, 328.
(22) Huber, K. P.; Herzberg. G. Constants of Diatomic Molecules. In *Molecular Spectra and Molecular Structure*; Van Nostrand Reinhold: New York, 1979; Vol. 4.
(23) Becke, A. D. *Phys. Rev.* **1988**, *A38*. 3098. Becke, A. D. *J. Chem. Phys.* **1993**, *98*, 1372. Becke, A. D. *J. Chem. Phys.* **1993**, *98*, 5648.
(24) Barone, V. M.; Cossi, M. *J. Phys. Chem. A* **1998**, *102*, 1995−2001.
(25) Barone, V. M.; Cossi, M.; Tomasi, J. *J. Chem. Phys.* **1997**, *107*, 3210−3221.
(26) Blomberg, M. R. A.; Siegbahn, P. E. M.; Babcock, G. T. *J. Am. Chem. Soc.* **1998**, *120*, 8812−8824.
(27) Siegbahn, P. E. M.; Blomberg, M. R. A. *Annu. Rev. Phys. Chem.* **1999**, *50*, 221−249.
(28) Siegbahn, P. E. M.; Blomberg, M. R. A. *Chem. Rev.* **2000**, *100*, 421−437.
(29) Siegbahn, P. E. M.; Blomberg, M. R. A. *J. Phys. Chem.* **2001**, *105*, 9375−9386.
(30) Frisch, M. J.; Trucks, G. W.; Schlegel, H. B.; Scuseria, G. E.; Robb, M. A.; Cheeseman, J. R.; Zakrzewski, V. G.; Montgomery, J. A.; Stratmann, R. E.; Burant, J. C.; Dapprich, S.; Millam, J. M.; Daniels, A. D.; Kudin, K. N.; Strain, M. C.; Farkas, O.; Tomasi, J.; Barone, V.; Cossi, M.; Cammi, R.; Mennucci, B.; Pomelli, C.; Adamo, C.; Clifford, S.; Ochterski, J.; Petersson, G. A.; Ayala, P. Y.; Cui, Q.; Morokuma, K.; Malick, D. K.; Rabuck, A. D.; Raghavachari, K.; Foresman, J. B.; Cioslowski, J.; Ortiz, J. V.; Stefanov, B. B.; Liu, G.; Liashenko, A.; Piskorz, P.; Komaromi, I.; Gomperts, R.; Martin, R. L.; Fox, D. J.; Keith, T.; Al-Laham, M. A.; Peng, C. Y.; Nanayakkara, A.; Gonzalez, C.; Challacombe, M.; Gill, P. M. W.; Johnson, B. G.; Chen, W.; Wong, M. W.; Andres, J. L.; Head-Gordon, M.; Replogle, E. S.; Pople, J. A. Gaussian, Inc.: Pittsburgh, PA, 1998.
(31) Hecht, H. J.; Kalisz, H. M.; Hendle, J.; Schmid, R. D.; Schomburg, D. *J. Mol. Biol.* **1993**, *229*, 153.
(32) Su, Q.; Klinman, J. P. *Biochemistry* **1999**, *38*, 8572.
(33) Roth, J. P.; Klinman, J. P. *J. Inorg. Biochem.* **2001**, *86*, 408.
(34) Langhoff, S. R.; Kern, C. W. *Modern Theoretical Chemistry*; Plenum Press: New York, 1977; p 381
(35) Minaev, B. F.; Lunell, S. *Z. Physik. Chemie* **1993**, *182*, 263.
(36) Condon, E. H.; Shortley, G. *Theory of Atomic Spectra*; Cambridge University Press: London, 1935.
(37) McGlynn, S. P.; Azumi, T.; Kinoshita, M. *Molecular Spectroscopy of the Triplet State*; Prentice Hall: Engelwood Cliffs, New Jersey, 1969.
(38) Minaev, B. F. *Fizika Molecul. Naukova Dumka, Kiev* **1979**, *7*, 34.
(39) Lorquet, A. J.; Lorquet, J. C.; Forst, W. *Chem. Phys.* **1980**, *51*, 241.
(40) Klessinger, M.; Michl, J. *Excited States and Photochemistry of Organic Molecules*; VCH: New York, 1995.
(41) Gemein, B.; Peyerimhoff, S. D. *J. Phys. Chem. A* **1996**, *100*, 19257.
(42) Turro, N. J. *Modern Molecular Photochemistry*; Benjamin: Menlo Park, CA, 1978.
(43) Ågren, H.; Vahtras, O.; Minaev, B. F. *Adv. Quantum Chem.* **1996**, *27*, 71.
(44) Minaev, B. F.; Vahtras, O.; Ågren, H. *Chem. Phys.* **1996**, *208*, 299.
(45) Gel'mukhanov, F. Kh.; Privalov, T. I.; Ågren, H. *Phys. Rev. A: At., Mol., Opt. Phys.* **1997**, *56*, 256.